


 Cite this: *RSC Adv.*, 2025, 15, 49959

Regio- and stereo-specific electrophilic addition of TeBr_4 and ArylTeBr_3 across terminal acetylene bonds

 Puspendra Singh, ^a Swami Nath Bharti, ^b Andrew Duthie ^c
 and Ray J. Butcher ^d

Despite their unique electronic properties and scope for use in applications including semiconductors, catalysis, materials science and medicine, organotellurium compounds remain underexplored. Hence, electrophilic addition reactions of TeBr_4 , $\text{C}_6\text{H}_5\text{TeBr}_3$, $4\text{-MeOC}_6\text{H}_4\text{TeBr}_3$ and $1\text{-C}_{10}\text{H}_7\text{TeBr}_3$ with terminal acetylene bonds of $\text{RC}\equiv\text{CH}$ ($\text{R} = \text{Me}_3\text{C}$, C_6H_5 , $4\text{-MeC}_6\text{H}_4$) were performed, producing the respective (*Z*)-isomer of organotellurium(IV) derivatives [*t*-BuC(Br)=CH]₂TeBr₂ (**1**), [(C₆H₅)-*t*-BuC(Br)=CH]TeBr₂ (**2**), [(4-MeOC₆H₄)-*t*-BuC(Br)=CH]TeBr₂ (**3**), [(1-C₁₀H₇)-*t*-BuC(Br)=CH]TeBr₂ (**4**), [(4-MeOC₆H₄)-(C₆H₅C(Br)=CH)]TeBr₂ (**5**), [(1-C₁₀H₇)-(C₆H₅C(Br)=CH)]TeBr₂ (**6**), [(C₆H₅)-(4-MeC₆H₄C(Br)=CH)]TeBr₂ (**7**), [(4-MeOC₆H₄)-(4-MeC₆H₄C(Br)=CH)]TeBr₂ (**8**) and [(1-C₁₀H₇)-(4-CH₃-C₆H₄C(Br)=CH)]TeBr₂ (**9**) in good yield. These derivatives were characterized by elemental analysis, ¹H, ¹³C{¹H} and ¹²⁵Te{¹H} NMR spectroscopic techniques. ¹H NMR chemical shifts of the signals due to vinyl protons of compounds **1–4** are shifted ~0.4 ppm up field due to the electronic effect of *t*-Bu group. Only one ¹²⁵Te NMR signal is observed for all the derivatives. Among these compounds, **2** and **7** were also characterized by single crystal X-ray studies. The Br atom of the organotellurium(IV) derivatives is invariably involved, at least in the solid state through nonbonding and hydrogen bonding interactions. An intermolecular Te...Br nonbonding interaction gives rise to zero-dimensional supramolecular dimeric unit in the crystal lattice of **2** and **7**.

 Received 18th September 2025
 Accepted 9th December 2025

DOI: 10.1039/d5ra07072d

rsc.li/rsc-advances

Introduction

Electrophilic addition reaction of alkynes is a highly valuable method for preparing alkanes, haloalkanes, haloalkenes, aldehydes, ketones, *cis*-alkenes, and *trans*-alkenes, *etc.*, due to the availability of loosely held π -electrons. This unique property of alkynes was first employed by Nicola Petragnani in the electrophilic addition reactions of TeCl_4 with phenylacetylene and diphenylacetylene.¹ Comasseto *et al.* have also demonstrated the addition reactions of arylTeCl₃ with 1-alkynes to isolate organotellurium(IV) derivatives.² The electrophilic addition reactions of TeBr_4 , arylTeBr₃ and phenylTeI₃ with a series of 1-alkynes, yielded the 1 : 1 addition products, respectively.^{3,4} The addition products formed can readily be reduced to β -bromo/iodovinyltellurides. Considering vinyl bromides are promising synthetic intermediates that can undergo many coupling reactions under the catalysis of transition metal complexes, the

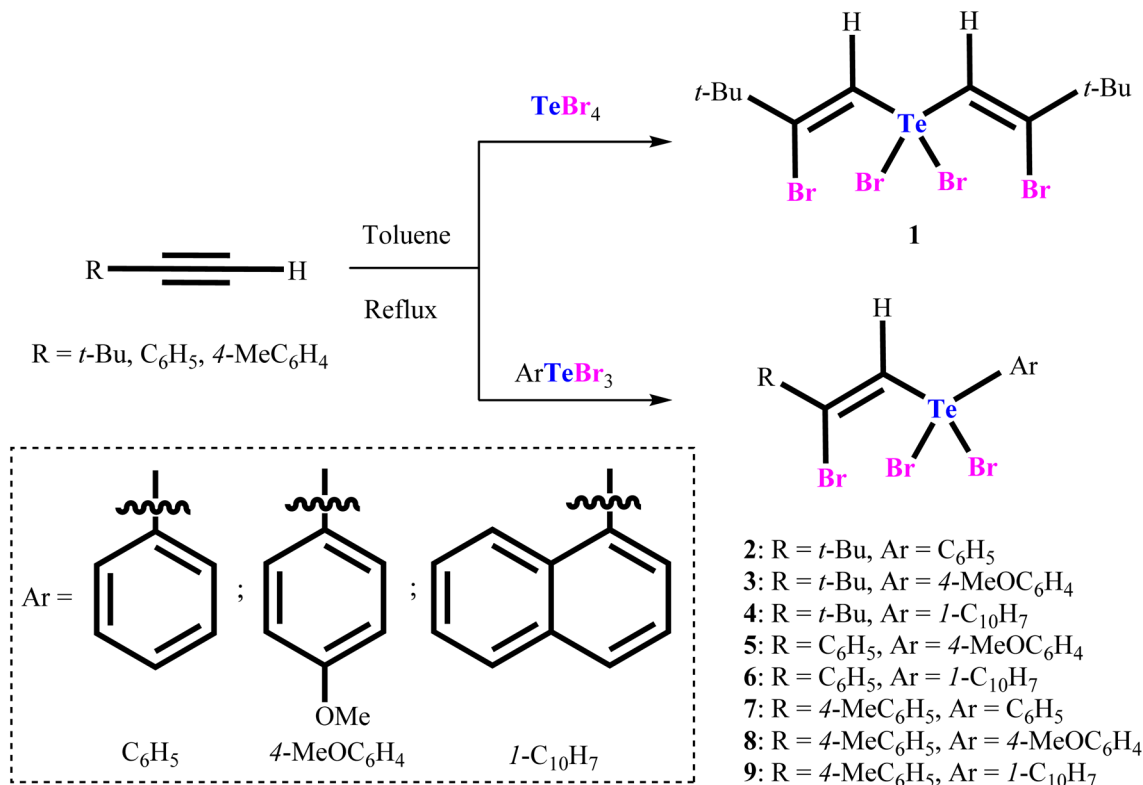
reaction assumes significance as it provides a stereoselective synthetic route to obtain β -bromovinyltellurides.⁵ The addition of tellurium(IV) tetra- or trihalides to terminal acetylenes was found to be highly regio- and stereoselective. A polar solvent, like methanol, that facilitates the formation of an intermediate telluronium ion, favored the anti-addition to afford the *E*-isomer. However, in a non-polar solvent like benzene, syn-addition reactions lead to *Z*-isomers *via* a four-membered cyclic transition state.^{6–8} Organotellurium(II) bromides and iodides that have appreciably low electrophilicity owing to the presence of two lone pairs at the Te(II) atom compared to their Te(IV) analogues have been demonstrated to undergo 1 : 1 addition reaction with terminal acetylenes and thus provide one-step access to β -halovinyltellurides in satisfactory yield.^{9,10} However, the regio- as well as stereo-selectivity of the addition reaction of Te(II) reagents to a triple bond was found to be poor and appeared to depend upon the reaction temperature and nature of the organic substrate. Thus, while the addition of phenyl tellurium bromide to phenylacetylene and *n*-heptyne gives the tellurides with *E*-configuration as the primary product at reflux, it yields its *Z*-isomers along with small amounts of regioisomers. TeCl_4 and arylTeCl₃ (Aryl = 1-C₁₀H₇, 2,4,6-Me₃C₆H₂, 4-MeOC₆H₄) can also be employed to add across the triple bond of 1-alkynes, $\text{RC}\equiv\text{CH}$ ($\text{R} = \text{Ph}$, 4-MeC₆H₄, *t*-Bu),

^aDepartment of Chemistry, Dr Shakuntala Misra National Rehabilitation University, Lucknow, 226017, India. E-mail: pushpendrasingh0612@gmail.com

^bDepartment of Chemistry, University of Lucknow, Lucknow, 226007, India

^cSchool of Life and Environmental Sciences, Deakin University, Geelong, 3217, Australia

^dDepartment of Chemistry, Howard University, Washington DC 20059, USA

Scheme 1 Synthesis of $[t\text{-BuC}(\text{Br})=\text{CH}]_2\text{TeBr}_2$ and $[t\text{-BuC}(\text{Br})=\text{CH}]\text{ArTeBr}_2$.

yielding the bis(2-chloro-2-phenylvinyl)tellurium dichloride or aryl(2-chloro-2-phenylvinyl)tellurium dichlorides, respectively.¹¹ The addition reactions of arylTeBr_3 with alkynes can be used to develop stereoselective synthesis of (*Z*)- or (*E*)- β -bromovinyl aryltellurium dibromides. Stereochemistry and the nature of the solvent were established in this report.¹² The addition reactions of TeBr_4 , alkylTeBr_3 and arylTeBr_3 with terminal acetylenes can be employed to isolate the corresponding bis(β -bromovinyl)tellurium dibromides and (β -bromovinyl)organyl tellurium dibromides.¹³ Similarly, ferrocenylacetylene can also react with a series of organotellurium(IV) tribromide/triiodide, affording (*Z*)-products of ferrocenylacetylene fragment bearing organotellurium(IV) derivatives respectively.¹⁴ In 2015, Chauhan and co-workers demonstrated the hydrotelluration of acetylenic ester using $\text{Ar}_2\text{Te}_2/\text{NaBH}_4$ ($\text{Ar} = 2,4,6\text{-Me}_3\text{C}_6\text{H}_2, 4\text{-Me}_2\text{NC}_6\text{H}_4$) in methanol, leading to a mixture of stereoisomers of methyl β -(aryltelluro)acrylates.¹⁵ Recently, addition of TeCl_4 to phenyl propargyl ethers was reported *via* anti addition following anti-Markovnikov rule to isolate bicyclic organotellurium derivatives.¹⁶ In 2024 Junk and co-workers also demonstrated synthesis of 1,3-benzotellurazole derivatives from phenyl ureas and tellurium tetrachloride.¹⁷ In addition, the same research group isolated 2-arylbenzo-1,3-tellurazoles from bis(2-aminophenyl) ditelluride and aromatic aldehydes by oxidative cyclization.¹⁸ Simultaneously, a review documented the synthesis and chemical behavior of telluropyran and telluropyrylium derivatives.¹⁹ The synthesis, ambient condition isolation, and antioxidant properties of a nine coordinate

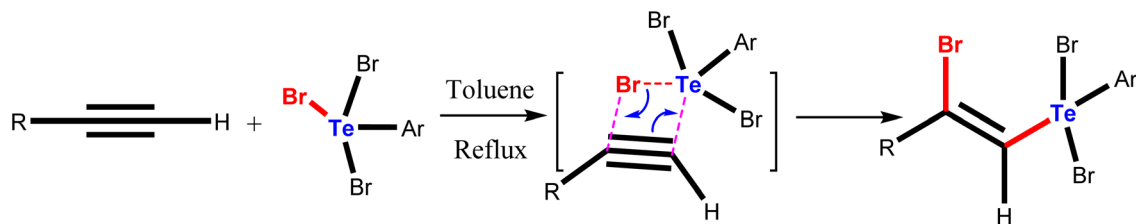
copper complex of 4-dimethylaminopyridyltellurium compound has also been performed.²⁰

Overall, organotellurium derivatives are generating significant interest due to their electronic properties and potential application in fields such as medicine, catalysis, and materials science. In light of this, we performed electrophilic addition reactions of TeBr_4 with *tert*-butylacetylene to obtain $[t\text{-BuC}(\text{Br})=\text{CH}]_2\text{TeBr}_2$ (**1**) with 66% yield. Along with this, $\text{C}_6\text{H}_5\text{TeBr}_3$, $4\text{-MeOC}_6\text{H}_4\text{TeBr}_3$ and $1\text{-C}_{10}\text{H}_7\text{TeBr}_3$ were also treated with terminal acetylene bonds of $\text{RC}\equiv\text{CH}$ ($\text{R} = \text{Me}_3\text{C}, \text{C}_6\text{H}_5, 4\text{-MeC}_6\text{H}_4$) to obtain the (*Z*)-isomer of unsymmetrical organotellurium(IV) derivatives, $[(\text{C}_6\text{H}_5)\text{-}t\text{-BuC}(\text{Br})=\text{CH}]\text{TeBr}_2$ (**2**), $[(4\text{-MeOC}_6\text{H}_4)\text{-}t\text{-BuC}(\text{Br})=\text{CH}]\text{TeBr}_2$ (**3**), $[(1\text{-C}_{10}\text{H}_7)\text{-}t\text{-BuC}(\text{Br})=\text{CH}]\text{TeBr}_2$ (**4**), $[(4\text{-MeOC}_6\text{H}_4)\text{-}(\text{C}_6\text{H}_5\text{C}(\text{Br})=\text{CH})]\text{TeBr}_2$ (**5**), $[(1\text{-C}_{10}\text{H}_7)\text{-}(\text{C}_6\text{H}_5\text{C}(\text{Br})=\text{CH})]\text{TeBr}_2$ (**6**), $[(\text{C}_6\text{H}_5)\text{-}(4\text{-MeC}_6\text{H}_4\text{-C}(\text{Br})=\text{CH})]\text{TeBr}_2$ (**7**), $[(4\text{-MeOC}_6\text{H}_4)\text{-}(4\text{-MeC}_6\text{H}_4\text{C}(\text{Br})=\text{CH})]\text{TeBr}_2$ (**8**) and $[(1\text{-C}_{10}\text{H}_7)\text{-}(4\text{-MeC}_6\text{H}_4\text{C}(\text{Br})=\text{CH})]\text{TeBr}_2$ (**9**) respectively. Compounds **2** and **7** were also examined further by single-crystal X-ray studies (Scheme 1).

Results and discussion

Phenyl, 4-tolyl and *t*-butylacetylenes undergo easy regio- and stereo-specific electrophilic addition reactions with TeBr_4 , $\text{C}_6\text{H}_5\text{TeBr}_3$, $4\text{-MeOC}_6\text{H}_4\text{TeBr}_3$ and $1\text{-C}_{10}\text{H}_7\text{TeBr}_3$ under refluxed in toluene, giving compounds **1–9** as solid yellow powders after work-up. The isolated pale yellow crystalline solids are air-stable, fairly soluble in chloroform or dichloromethane but sparingly soluble in benzene, *n*-hexane and ethers.



Scheme 2 Plausible mechanism for the formation of [RC(Br)=CH]ArTeBr₂.

Characterization and structural studies of the new compounds, *vide infra*, indicate that 1,2-addition of Te–Br bonds of TeBr₄ and more reactive equatorial Te–Br bonds of ArTeBr₃ across a triple bond of 1-alkynes in toluene is regio- and stereospecific and proceeds *via* a concerted four-centered mechanism to give the (*Z*) isomer (Scheme 2).²¹

Spectroscopic studies

All the compounds are crystalline solids and sufficiently soluble in CDCl₃ to obtain satisfactory NMR spectra. ¹H NMR chemical shifts of the signals due to vinyl protons of compounds 1–4 are shifted ~0.4 ppm up field due to electronic effects of the *t*-Bu group. The ¹H NMR spectrum of compound 1 shows two singlets at 1.31 and 7.86 ppm for *t*-Bu and vinyl protons,

respectively. The ¹H NMR spectrum of 2 shows two singlets at 1.31 and 7.78 ppm for *t*-Bu and vinyl protons. Along with these singlets, we also observed two sets of multiplets at 7.50–7.55 and 8.25–8.28 ppm for phenyl protons. The ¹H NMR spectrum of compound 3 shows three singlets at 1.30, 3.87 and 7.74 ppm for *t*-Bu, *p*-MeO and vinyl protons, respectively. Along with these singlets, two sets of doublets are also observed at 7.02–7.05 and 8.16–8.19 ppm for aryl protons with a coupling constant 9.0 Hz. The ¹H NMR spectrum of compound 4 shows two singlets at 1.40 and 8.08 ppm for *t*-Bu and vinyl protons, respectively. Along with these singlets, three doublets and three multiplets are also observed for aryl protons with coupling constants 7.5 and 8.1 Hz. The ¹H NMR spectrum of 5 shows two singlets at 3.84 and 8.16 ppm for *p*-CH₃O and vinyl protons, respectively.

Table 1 Crystallographic data and structure refinement details for 2 and 7

	2	7
Formula	C ₁₂ H ₁₅ Br ₃ Te	C ₁₅ H ₁₃ Br ₃ Te
Formula weight	526.57	560.58
Temperature (K)	295(2)	295(2)
Wavelength, λ (Å)	0.71073	0.71073
Crystal system	Monoclinic	Triclinic
Space group	<i>P</i> 2 ₁ / <i>n</i>	<i>P</i> 1
<i>a</i> (Å)	8.1805(3)	8.1272(4)
<i>b</i> (Å)	19.8262(6)	13.6069(6)
<i>c</i> (Å)	9.5995(3)	17.3929(6)
α (°)	90	106.777(3) ^o
β (°)	98.090(3)	96.291(3)
γ (°)	90	106.069(4)
<i>V</i> (Å ³)	1541.43(9)	1731.66(14)
<i>Z</i>	4	4
ρ _{calcd} (Mg m ⁻³)	2.269	2.150
Abs coeff. (mm ⁻¹)	9.681	8.625
<i>F</i> (000)	976	1040
Crystal size (mm ³)	0.73 × 0.28 × 0.07	0.78 × 0.59 × 0.21
θ Range (°)	3.07 to 40.96	1.65 to 26.32
Index ranges	−14 ≤ <i>h</i> ≤ 14 −36 ≤ <i>k</i> ≤ 35 −17 ≤ <i>l</i> ≤ 16	−9 ≤ <i>h</i> ≤ 10 −16 ≤ <i>k</i> ≤ 15 −13 ≤ <i>l</i> ≤ 21
Reflns collected	19 655	11 387
Indep reflns	9887 [<i>R</i> (int) = 0.0438]	6769 [<i>R</i> (int) = 0.0448]
Completeness to θ max (%)	99.9	99.6
Abs. correction	Analytical	Analytical
Max., min. transmission	0.505, 0.049	0.133, 0.009
Data/restraints/params	9887/0/148	6769/61/377
GoF (<i>F</i> ²)	1.037	1.096
Final <i>R</i> indices [<i>I</i> > 2σ(<i>I</i>)]	<i>R</i> 1 = 0.0517, <i>wR</i> 2 = 0.0683	<i>R</i> 1 = 0.0466, <i>wR</i> 2 = 0.1244
<i>R</i> indices (all data)	<i>R</i> 1 = 0.1032, <i>wR</i> 2 = 0.0833	<i>R</i> 1 = 0.0517, <i>wR</i> 2 = 0.1287
Refinement method	Full-matrix least-squares on <i>F</i> ²	
Larg. diff. peak/hole (e Å ⁻³)	1.811/−2.954	1.184/−0.918



Table 2 Hydrogen-bonds for 2 and 7 [Å and °]

	D–H...A	<i>d</i> (D–H)	<i>d</i> (H...A)	<i>d</i> (D...A)	∠(D–H...A)	Symmetry
2	C2–H2A...Br1	0.93	3.095(0)	3.717(3)	125.8	1 + <i>x</i> , <i>y</i> , + <i>z</i>
	C3–H3A...Br2	0.93	3.049(0)	3.609(3)	120.4	1 – <i>x</i> , 1 – <i>y</i> , 1 – <i>z</i>
7	C8B–HBA...Br2B	0.93	3.184(1)	3.996(7)	147.0	2 – <i>x</i> , 1 – <i>y</i> , 1 – <i>z</i>
	C14B–H14B...Br1A	0.93	3.049(1)	3.833(8)	142.9	2 – <i>x</i> , 1 – <i>y</i> , 1 – <i>z</i>
	C15A–H15A...Br2B	0.96	3.087(1)	3.875(7)	143.6	2 – <i>x</i> , 1 – <i>y</i> , 1 – <i>z</i>

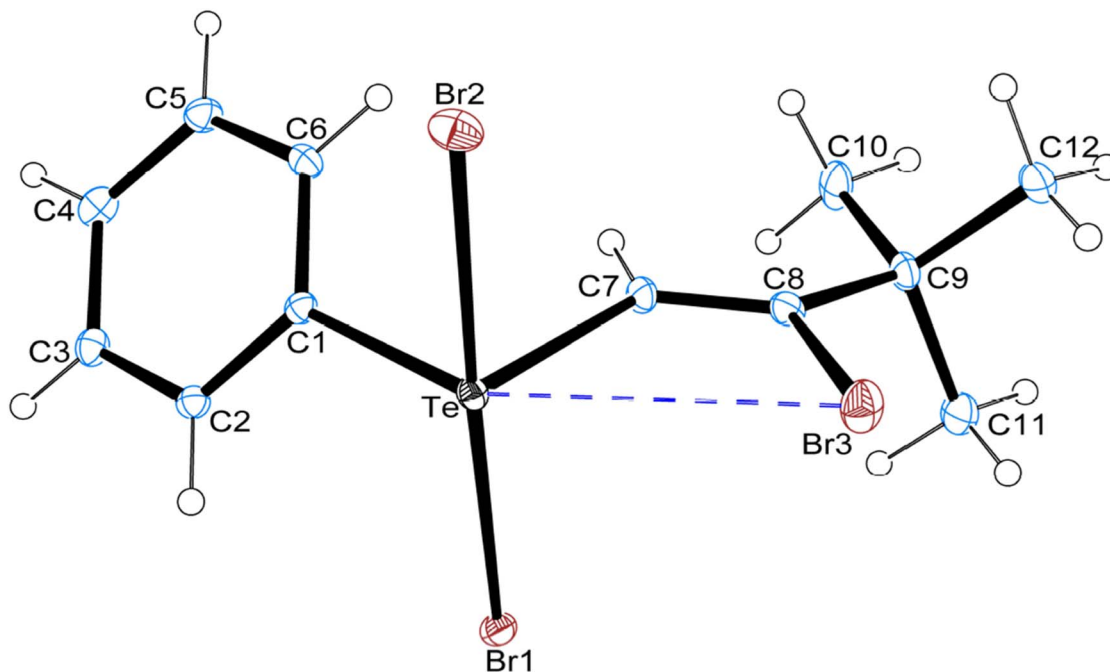


Fig. 1 ORTEP diagram showing 30% probability displacement ellipsoids and crystallographic numbering scheme for 2. Selected bond distances (Å) and angles (°): Te–C(1): 2.125(3); Te–C(7): 2.099(3); C(8)–Br(3): 1.915(3); Te–Br(1): 2.7193(4); Te–Br(2): 2.6379(4); Te...Br(3): 3.3734(11); C(1)–Te...Br(3): 148.33(8); C(1)–Te–C(7): 93.13(11); Br(1)–Te–Br(2): 176.839(13); τ : 176.84–93.13/60 = 1.39.

Along with these singlets, in the aryl region we also observed to have two doublet of doublets with coupling constants 9.0 and 3.0 Hz and three multiplets. The ^1H NMR spectrum of 6 shows a singlet at 8.45 ppm for the vinyl proton, three multiplets and three doublets with a coupling constant 8.1 Hz. The ^1H NMR spectrum of 7 shows two singlets at 2.40 and 8.14 ppm for *p*-Me and vinyl protons, respectively. Along with these singlets, the aryl region shows two multiplets and a doublet with a coupling constant 9.6 Hz. The ^1H NMR spectrum of 8 shows three singlets at 2.40, 3.88 and 8.10 ppm for *p*-Me, *p*-MeO and vinyl protons, respectively. Along with these singlets, four doublets are also observed with coupling constants of 8.1 and 9.0 Hz. The ^1H NMR spectrum of 9 shows two singlets at 2.43 and 8.40 ppm for *p*-Me and vinyl protons, respectively. Along with these singlets, two multiples and four doublets are observed.

The $^{125}\text{Te}\{^1\text{H}\}$ NMR spectrum of compounds 1–9 exhibits a single resonance at 714.3, 795.2, 805.0, 697.7, 808.6, 759.4, 689.7, 811.4 and 706.3 ppm, respectively, suggesting their stability in the solution state. The observed $^{125}\text{Te}\{^1\text{H}\}$ NMR chemical shift in these compounds are very close to the reported $^{125}\text{Te}\{^1\text{H}\}$ NMR chemical shift for (1- C_{10}H_7)(*t*-BuCOCH₂)

TeCl₂ (762.6 ppm), (2,4,6-Me₃C₆H₂)(*t*-BuCOCH₂)TeCl₂ (814.5 ppm),²² (1- C_{10}H_7)(*i*-PrCOCH₂)TeCl₂ (760.1 ppm), (2,4,6-Me₃C₆H₂)(*i*-PrCOCH₂)TeCl₂ (780.8 ppm),²³ (2,4,6-Me₃C₆H₂)(Et₂NCOCH₂)TeBr₂ (745.0 ppm),²⁴ (MeOCOCH₂)₂TeBr₂, (748.0 ppm), (1- C_{10}H_7)(MeOCOCH₂)TeBr₂, (713.0 ppm) and (2,4,6-Me₃C₆H₂)(MeOCOCH₂)TeBr₂ (721.0 ppm).²⁵

Molecular and crystal structures of 2 and 7

The relevant individual crystals of compounds 2 and 7 suitable for X-ray studies were obtained by slow evaporation of their chloroform solutions at room temperature. Single-crystal X-ray data and structure refinement details are given in Table 1, while the hydrogen bonding interaction (HBIs) details are summarised in Table 2. ORTEP diagrams of 2 and 7 are depicted in Fig. 1 and 2, respectively. The crystal packing diagrams of their molecular structures are shown in Fig. S1–S2. Significant bond lengths and angles are depicted in the figure captions. Compound 2 crystallizes in monoclinic with $P2_1/n$ space group and compound 7 crystallizes in triclinic with $P\bar{1}$ space group. Crystal lattices of both compounds are centrosymmetric. In the case of 2, the asymmetric unit consists of one molecule, while in



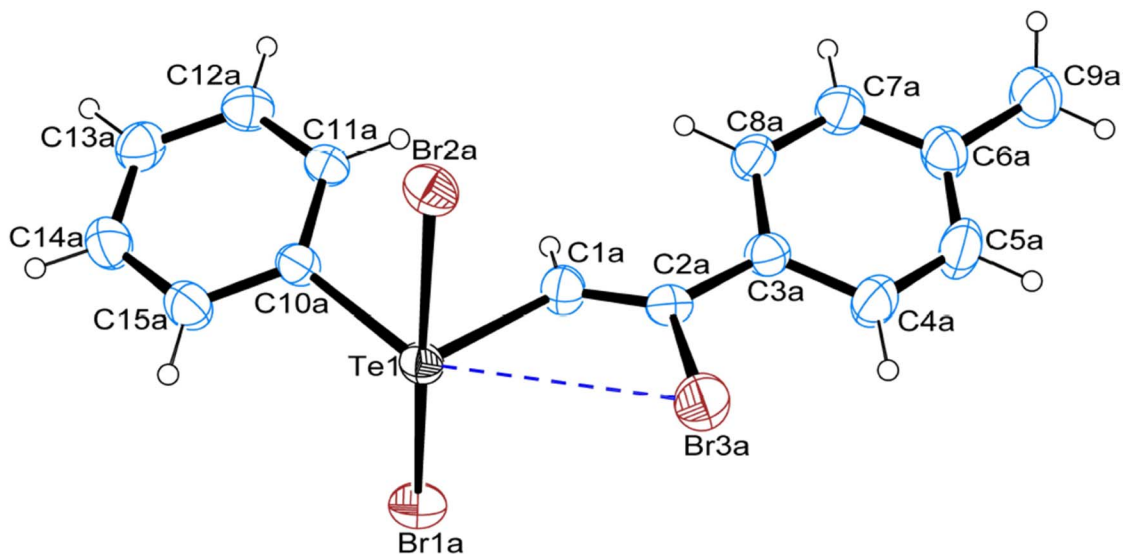


Fig. 2 ORTEP diagram showing 30% probability displacement ellipsoids and crystallographic numbering scheme for **7**. Selected bond distances (Å) and angles (°): Molecule A: Te(1)–C(1A): 2.086(6); Te–C(10A): 2.1075(6); C(2A)–Br(3A): 1.906(6); Te(1)–Br(1A): 2.6375(8); Te(1)–Br(2A): 2.7123(7); Te(1)⋯Br(3A): 3.373(1); C(10A)–Te(1)⋯Br(3A): 150.51(18); C(1A)–Te(1)–C(10A): 97.6(2); Br(1A)–Te(1)–Br(2A): 176.19(2); τ : 176.19–97.6/60 = 1.31. Molecule B: Te(2)–C(1B): 2.075(6); Te(2)–C(10B): 2.113(7); C(2B)–Br(3B): 1.901(9); Te(2)–Br(1B): 2.6504(12); Te(2)–Br(2B): 2.7242(11); Te(2)⋯Br(3B): 3.427(8); C(10B)–Te(2)⋯Br(3B): 146.91(31); C(1B)–Te(2)–C(10B): 95.3(3); Br(1B)–Te(2)–Br(2B): 177.74(3); τ : 177.74–95.3/60 = 1.37.

the case of **7**, there are two crystallographically independent molecules. Though the crystal structure of **2** is free from any disorder, the vinyl Br atom in one of the molecules of **7** is four-fold disordered with positional occupancies of 0.38(3) for

(Br3B), 0.39(3) for (Br3C), 0.09(3) for (Br3D), and 0.14(3) for (Br3E). The primary geometry around the Te(IV) atom in both compounds is pseudo-trigonal bipyramidal with one equatorial position occupied by a stereochemically active lone pair. The

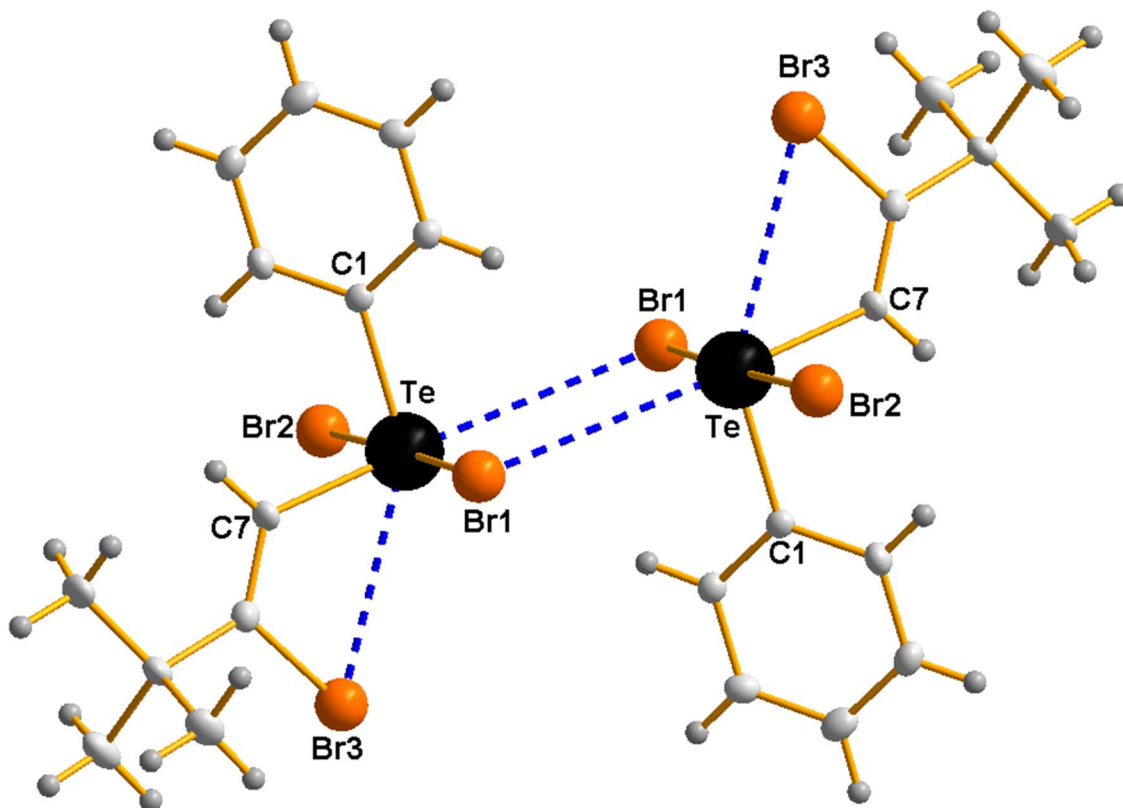


Fig. 3 Zero-dimensional supramolecular centrosymmetric dimeric unit sustained by Te⋯Br(lp) NBIs [Te⋯Br(1): 3.604(0); Te⋯Br(2): 3.542(1); Te⋯Br(3): 3.366(1) Å, C(1)–Te⋯Br(3): 148.33(8); C(7)–Te⋯Br(1): 166.98(8)°] in the crystal structure of **2**.



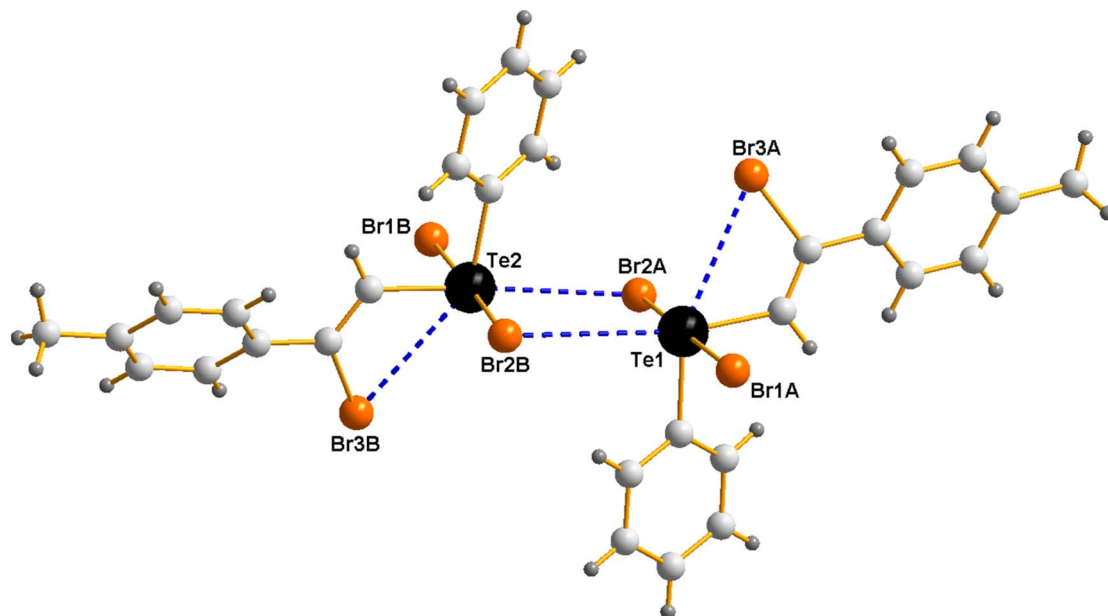


Fig. 4 Zero-dimensional supramolecular dimeric unit of molecules "A" and "B" of 7 in its crystal lattice realized through intermolecular Te...Br attractions. Centrosymmetric dimer sustained by Te...Br(lp) NBIs [Te(1)...Br(2B): 3.707(11); Te(2)...Br(2A): 3.542(1); Te(1)...Br(3A): 3.373(1); Te(2)...Br(3B): 3.427(8) Å, C(1A)–Te(1)...Br(2B): 170.02(18); C(10A)–Te(1)...Br(3A): 150.5(2); C(1B)–Te(2)...Br(2A): 175.64(18); C(10B)–Te(2)...Br(3B): 149.2(2)^o].

distorted geometries can also be confirmed with the observed tau parameters (τ) for 2 : 1.39 and for 7 : 1.37. Molecular structures of both compounds in the solid state contain the putative planar vinyl fragment, C(Br)C=C(H)Te. The observed C=C bond length of 1.316(4) Å for 2 and 1.3170(10), 1.325(13) Å for two independent molecules of 7 are comparable to the value (1.337 Å) in free ethylene. The ethylene fragment bound to the Te atom in both compounds displays (*Z*) stereochemistry. The observed intramolecular nonbonding interactions (NBIs) [Te...Br(3): 3.3734(11) for 2; Te(1)...Br(3A): 3.373(1) for molecule A and Te(2)...Br(3B): 3.427(8) Å for molecule B of 7] are longer than the $\Sigma r_{\text{cov}}(\text{Te}, \text{Br})$, 2.68 Å, and significantly shorter than $\Sigma r_{\text{vdw}}(\text{Te}, \text{Br})$, 4.04 Å.²⁶ In the face of possible rotations about the Te–C bonds, the vinyl fragment, C(Br)C=C(H)Te in both cases is orientated so that the bromine atom(s) are almost in the equatorial C–Te–C plane. Coplanarity together with near linearity of the Br...Te–C(*trans*) triad(s) ($\angle \text{Br}\cdots\text{Te}-\text{C}(\text{trans}) \sim 148^\circ$) make $n \rightarrow \sigma^*$ orbital interaction feasible.²⁷ The four-electron three-centre covalent bonding interaction, therefore, appears to be the major component of the attractive interaction between the lone pair-laden hypervalent Te(IV) and Br atoms.

Supramolecular aspects

The propensity exhibited by the central Te atom among organotellurium(IV) halides to achieve six-coordination *via* intra/intermolecular Te...A (A = an electron-rich p-block atom *viz.* O, N, Cl, Br, I) NBIs is well displayed in the crystal packings of 2 and 7 (Fig. S1–S2).²⁸ In the crystal lattice of compounds 2 and 7, as well, the intermolecular reciprocatory Te...Br NBIs imparts six-coordination to Te(IV) atom with pseudo-octahedral geometry and results in the formation of centrosymmetric dimeric

units (Fig. 3). The observed intermolecular NBIs [Te...Br(1): 3.604(0) for 2; Te(1)...Br(2B): 3.707(11) and Te(2)...Br(2A): 3.542(1) for 7] are longer than the $\Sigma r_{\text{cov}}(\text{Te}, \text{Br})$, 2.68 Å, and significantly shorter than $\Sigma r_{\text{vdw}}(\text{Te}, \text{Br})$, 4.04 Å.²⁶ Linearity of the Br...Te–C(*trans*) triad(s) [$\angle \text{C}(7)-\text{Te}\cdots\text{Br}(1)$: 166.98(8)^o for 2 and C(1A)–Te(1)...Br(2B): 170.02(18) for molecule A and C(1B)–Te(2)...Br(2A): 175.64(18) for molecule B of 7] approaching to 180^o to make $n \rightarrow \sigma^*$ orbital interaction feasible.²⁷ In compound 7, pairs of the independent molecules "A" and "B" form dimeric units through reciprocatory intermolecular Te...Br NBIs (Fig. 4). The crystal packing diagrams of 2 and 7, also sustained by numerous reciprocatory C–H...Br HBIs, give rise to a one-dimensional supramolecular self-assembly (Fig. S1 and S2).

Hirshfeld surface analysis

Hirshfeld surface (HS) analyses were carried out to gain deeper insight into the intermolecular interactions present in the crystal structure of complexes 2 and 7. The associated 2D fingerprint plots were generated using CrystalExplorer21.5 to demonstrate the relative contributions of all possible intermolecular HBIs and NBIs to the overall surface area (Fig. 5, for detailed breakdown see Fig. S3–S6). For the compounds under investigation, prominent red spots were observed near the Br atom in compounds 2 and 7, highlighting the key intermolecular interactions (Fig. 5). Among these interactions, the H...H and H...Br interactions are the most prominent, contributing 30.5–40.7%. The highest H...H (40.7%) and H...Br (39.8%) contribution is observed for complex 2 and complex 7, respectively, suggesting a densely packed structure. The H...Br interactions, arising from C–H...Br HBIs, with the highest value for



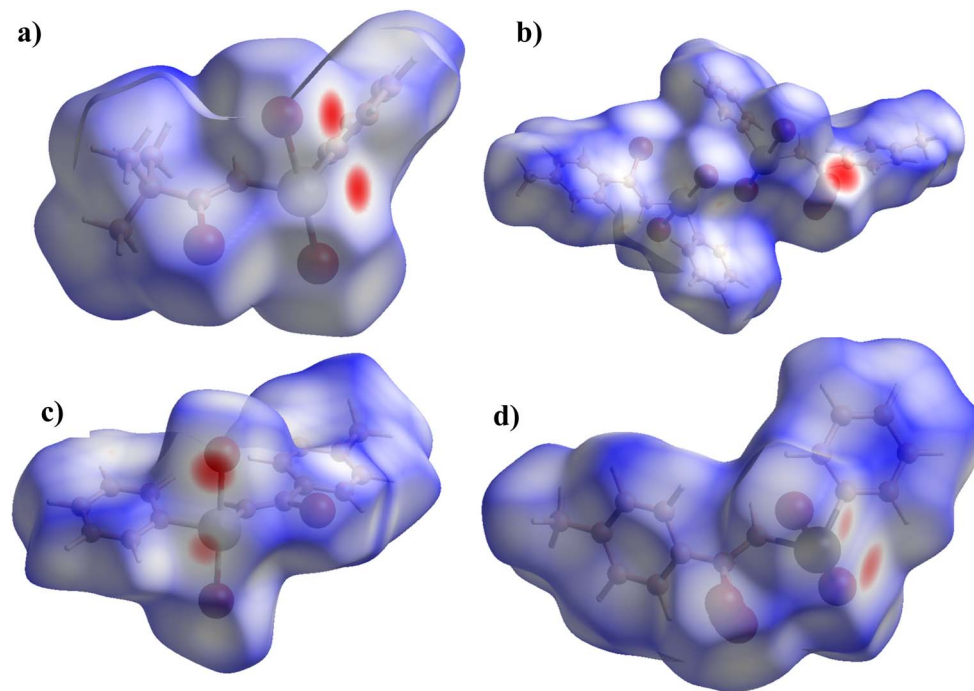


Fig. 5 Hirshfeld surfaces (mapped over d_{norm}). (a) Compound 2, (b) compound 7, (c) molecule A of compound 7, (d) molecule B of compound 7.

complex 7 (39.8%). The C \cdots H interactions represent the third significant contribution of 9.9% with complex 2 and 19.3%, with complex 7 exhibiting the highest proportion. These contacts are typically associated with C–H \cdots π and C–H \cdots C interactions. Along with these interactions Br \cdots Br and Te \cdots Br NBIs are also contributing. For compound 2, Br \cdots Br (5.9%) Te \cdots Br/Br \cdots Te (3.6%) and H \cdots Te/Te \cdots H (2.0%) contacts (Fig. S3). In compound 7, the corresponding contributions are Br \cdots Br (3.7%) and H \cdots Te/Te \cdots H (1.5%) contacts (Fig. S4). To gain deeper insight into the crystal structure of 7. Molecule A and B of compound 7 both separately studied with the help of HS analysis, revealed that the presence of Te \cdots Br NBIs with 2.3% contacts (Fig. S5 and S6). These results are consistent with the observed packing features and highlight the role of non-covalent interactions in stabilizing the crystal structures (please see SI File for Fig. S3–S6).

Experimental

General

All reactions were performed under dry nitrogen. The starting materials *tert*-butylacetylene, phenylacetylene, *p*-ethynyltoluene, TeBr₄, bromine, bromobenzene, 4-bromoanisole, 1-bromonaphthalene, bromomesityl, THF, toluene and chloroform were purchased from Merck and Aldrich. The starting materials C₆H₅TeBr₃,^{29,30} 4-MeOC₆H₄TeBr₃,^{29,30} and 1-C₁₀H₇TeBr₃ (ref. 30) were prepared according to literature methods. Melting points were recorded in capillary tubes and are uncorrected. The ¹H (300.13 MHz), ¹³C{¹H} (125.77 MHz) and ¹²⁵Te{¹H} (157.86 MHz) NMR spectrum were recorded in CDCl₃ on Bruker Avance 300 and 500 spectrometers. Chemical shifts cited were referenced to Me₄Si (¹H, ¹³C{¹H}) and Me₂Te

(¹²⁵Te). Elemental analyses were performed on a Carlo Erba model 1106 elemental analyzer.

Reaction of TeBr₄ and ArTeBr₃ with acetylenes

Compound 1 [*t*-BuC(Br)=CH]₂TeBr₂. A solution of *tert*-butylacetylene (0.62 mL, 5 mmol) and TeBr₄ (0.90 g, 2 mmol) in dry toluene (10 mL) was refluxed under stirring for 8 h. The completeness of the reaction was monitored through TLC, eluting with CHCl₃ : CH₃OH (9 : 1). The solvent was reduced to approximately one third under reduced pressure and petroleum ether 60–80 °C was added. The sticky mass so obtained, on trituration with petroleum ether (60–80 °C) afforded a light yellow solid. After decantation of the solvent, the solid was dissolved in chloroform and passed through a short silica column to remove elemental tellurium produced due to partial decomposition. The resulting filtrate was concentrated to give a yellow solid powder of **1**. The solid was recrystallized from chloroform to give yellow needle-shaped crystals of **1**. Yield: (0.87 g, 66%); mp 193 °C (from CHCl₃) (found: C, 23.24; H, 3.23. C₁₂H₂₀Br₄Te requires C, 23.57; H, 3.30%); ¹H NMR (ppm): 1.31 (9H, s, *t*-Bu), 7.86 (1H, s, vinyl). ¹³C{¹H} NMR, (ppm): 29.18 (*t*-Bu), 42.4, 122.4, 156.3 (vinyl). ¹²⁵Te{¹H} NMR (ppm): δ 714.3.

Compound 2 [(C₆H₅)-*t*-BuC(Br)=CH]₂TeBr₂. Prepared from C₆H₅TeBr₃ (0.89 g, 2.0 mmol) and *tert*-butylacetylene (0.62 mL, 5 mmol) at reflux, in a way similar to **1**. Yield: (0.68 g, 65%); mp 125 °C (from CHCl₃) (found: C, 27.42; H, 2.77. C₁₂H₁₅Br₃Te requires C, 27.37; H, 2.87%); ¹H NMR (ppm): 1.31 (9H, s, *t*-Bu), 7.50–7.55 (3H, m, aryl), 7.78 (1H, s, vinyl), 8.25–8.28 (2H, m, aryl). ¹³C{¹H} NMR (ppm): 29.3 (*t*-Bu), 42.4, 126.0, 156.6 (vinyl), 130.4, 131.9, 135.0 (aryl). ¹²⁵Te{¹H} NMR (ppm): 795.2.

Compound 3 [(4-MeOC₆H₄)-*t*-BuC(Br)=CH]₂TeBr₂. Prepared from 4-MeOC₆H₄TeBr₃ (0.95 g, 2.0 mmol) and *tert*-



butylacetylene (0.62 mL, 5 mmol) at reflux, in a way similar to **1**. Yield: (0.67 g, 60%); mp 143 °C (from CHCl₃) (found: C, 4, 28.10; H, 3.12). C₁₃H₁₇Br₃OTe requires C, 28.05; H, 3.08%; ¹H NMR (ppm): 1.30 (9H, s, *t*-Bu), 3.87 (3H, s, CH₃O), 7.02–7.05 (2H, d *J* 9.0 Hz, aryl), 7.74 (1H, s, vinyl), 8.16–8.19 (2H, d *J* 9.0 Hz, aryl). ¹³C{¹H} NMR (ppm): 29.2 (*t*-Bu), 42.3, 55.8 (CH₃O), 116.1, 156.4 (vinyl), 119.2, 126.3, 136.8, 162.3 (aryl). ¹²⁵Te{¹H} NMR (ppm): 805.0.

Compound 4 [(1-C₁₀H₇)-(t-BuC(Br)=CH)]TeBr₂. Prepared from 1-C₁₀H₇TeBr₃ (0.99 g, 2.0 mmol) and *tert*-butylacetylene (0.62 mL, 5 mmol) at reflux, in a way similar to **1**. Yield: (0.83 g, 72%); mp 188 °C (from CHCl₃) (found: C, 33.08; H, 2.89). C₁₆H₁₇Br₃Te requires C, 33.33; H, 2.97%; ¹H NMR (ppm): 1.40 (9H, s, *t*-Bu), 7.60–7.67 (2H, m, aryl), 7.69–7.74 (1H, m, aryl), 7.95–7.98 (1H, d *J* 8.1 Hz, aryl), 8.05–8.09 (2H, m, aryl), 8.27–8.30 (1H, d *J* 7.5 Hz, aryl), 8.08 (1H, s, vinyl), 8.27–8.30 (1H, d *J* 7.5 Hz, aryl). ¹³C{¹H} NMR (ppm): 29.3 (*t*-Bu), 42.6, 124.1, 156.5 (vinyl), 126.9, 127.0, 127.6, 128.2, 129.6, 131.6, 132.8, 132.8, 134.7 (aryl). ¹²⁵Te{¹H} NMR (ppm): 697.7.

Compound 5 [(4-MeOC₆H₄)-(C₆H₅C(Br)=CH)]TeBr₂. Prepared from 4-MeOC₆H₄TeBr₃ (0.95 g, 2.0 mmol) and phenylacetylene (0.55 mL, 5 mmol) at reflux in a way similar to **1**. Yield: (0.90 g, 78%); mp 155 °C (from CHCl₃) (found: C, 31.20; H, 2.28). C₁₅H₁₃Br₃OTe requires C, 31.25; H, 2.27%; ¹H NMR (ppm): 3.84 (3H, s, OMe), 7.02–7.08 (2H, dd *J* 9.0 Hz & 3.0 Hz, anisyl), 7.38–7.47 (3H, m, phenyl), 7.62–7.67 (2H, m, phenyl), 8.16 (1H, s, vinyl), 8.21–8.26 (2H, dd *J* 9.0 & 3.0 Hz, anisyl). ¹²⁵Te{¹H} NMR (ppm): 808.6.

Compound 6 [(1-C₁₀H₇)-(C₆H₅C(Br)=CH)]TeBr₂. Prepared from 1-C₁₀H₇TeBr₃ (0.99 g, 2.0 mmol) and phenylacetylene (0.55 mL, 5 mmol) at reflux in a way similar to **1**. Yield: (1.01 g, 84%); mp 183 °C (from CHCl₃) (found: C, 36.24; H, 2.60). C₁₈H₁₃Br₃Te requires C, 36.24; H, 2.20%; ¹H NMR (ppm): 7.43–7.49 (3H, m, aryl), 7.62–7.67 (2H, m, aryl), 7.71–7.77 (3H, m, aryl), 7.96–7.99 (1H, d *J* 8.1 Hz, aryl), 8.08–8.10 (2H, d *J* 8.1 Hz, aryl), 8.37–8.40 (1H, d *J* 7.5 Hz, aryl), 8.45 (1H, s, vinyl). ¹³C{¹H} NMR (ppm): 67.3, 123.6, 126.6, 126.7, 126.9, 127.4, 128.8, 129.5, 131.4, 131.5, 132.1, 132.8, 134.4, 134.5, 135.3, 135.9 (aryl), 192.1 (vinyl). ¹²⁵Te{¹H} NMR (ppm): 759.4.

Compound 7 [(C₆H₅)-(4-MeC₆H₄C(Br)=CH)]TeBr₂. Prepared from C₆H₅TeBr₃ (0.89 g, 2.0 mmol) and *p*-ethynyltoluene (0.63 mL, 5 mmol) at reflux in a way similar to **1**. Yield: (0.63 g, 56%); mp 77 °C (from CHCl₃) (found: C, 31.98; H, 2.40). C₁₅H₁₃Br₃Te requires C, 32.14; H, 2.34%; ¹H NMR (ppm): 2.40 (3H, s, *p*-Me), 7.17–7.20 (2H, d *J* 9.6 Hz, *m*-tolyl), 7.52–7.57 (5H, m, phenyl), 8.14 (1H, s, vinyl), 8.30–8.33 (2H, m, *o*-tolyl). ¹³C{¹H} NMR (ppm): 21.6 (*p*-Me), 125.3, 128.3, 129.6, 130.5, 132.0, 133.6, 135.0, 141.1 (aryl), 142.2, (vinyl). ¹²⁵Te{¹H} NMR (ppm): 689.7.

Compound 8 [(4-MeOC₆H₄)-(4-MeC₆H₄C(Br)=CH)]TeBr₂. Prepared from 4-MeOC₆H₄TeBr₃ (0.95 g, 2.0 mmol) and *p*-ethynyltoluene (0.63 mL, 5 mmol) at reflux in a way similar to **1**. Yield: (0.91 g, 77%); mp 156 °C (from CHCl₃) (found: C, 32.61; H, 2.60). C₁₆H₁₅Br₃OTe requires C, 32.54; H, 2.56%; ¹H NMR (ppm): 2.40 (3H, s, *p*-Me), 3.88 (3H, s, MeO), 7.03–7.06 (2H, d *J* 9.0 Hz, *o*-anisyl), 7.19–7.22 (2H, d *J* 8.1 Hz, *o*-tolyl); 7.51–7.54 (2H, d *J* 8.1 Hz, *m*-tolyl), 8.10 (1H, s, vinyl), 8.22–8.24 (2H, d *J* 9.0 Hz, *m*-anisyl). ¹³C{¹H} NMR (ppm): 21.6 (*p*-Me), 55.8 (*p*-

MeO), 116.1, 125.8, 128.2, 129.6, 133.6, 136.8, 140.8, 142.1 (aryl), 162.4, (vinyl). ¹²⁵Te{¹H} NMR (ppm): 811.4.

Compound 9 [(1-C₁₀H₇)-(4-CH₃-C₆H₄C(Br)=CH)]TeBr₂. Prepared from 1-C₁₀H₇TeCl₃ (0.99 g, 2.0 mmol) and *p*-ethynyltoluene (0.63 mL, 5 mmol) at reflux in a way similar to **1**. Yield: (0.78 g, 63%); mp 170 °C (from CHCl₃) (found: C, 37.34; H, 2.53). C₁₉H₁₅Br₃Te requires C, 37.37; H, 2.48%; ¹H NMR (ppm): 2.43 (3H, s, *p*-Me), 7.24–7.26 (1H, d *J* 4.8 Hz, aryl), 7.60–7.67 (4H, m, aryl), 7.71–7.76 (1H, m, aryl), 7.96–7.98 (1H, d *J* 8.1 Hz, aryl), 8.07–8.09 (2H, d *J* 7.8 Hz, aryl), 8.36–8.39 (1H, d *J* 7.2 Hz, aryl), 8.40 (1H, s, vinyl). ¹³C{¹H} NMR (ppm): 21.6 (*p*-Me), 123.4, 126.9, 127.0, 127.6, 128.2, 128.3, 129.7, 131.6, 132.9, 133.0, 133.9, 134.8, 141.0 (aryl) 142.2 (vinyl). ¹²⁵Te{¹H} NMR (ppm): 706.3.

Crystallography

A suitable-sized single crystal was selected using an optical microscope and attached on the top of a glass fiber for data collection. Intensity data of the molecules were recorded using MoK α ($\lambda = 0.71073$ Å) radiation on a Bruker SMART APEX diffractometer with a CCD area detector at 295(2) K. The data was integrated with SAINT software³¹ and an experimental absorption correction applied to the collected reflections with SADABS.³² The structure was confirmed by direct methods using SHELXTL and refined on F2 by the full-matrix least-squares procedure using the program SHELXL-2018.³³ All non-hydrogen atoms were refined with anisotropic displacement parameters, whereas all H atoms were positioned geometrically and refined with relative isotropic displacement parameters. ORTEP and packing diagrams are generated with the ORTEP-3,³⁴ and DIAMOND 3.2 programs, respectively.³⁵ Hirshfeld surface (HS) analyses and associated 2D fingerprint plots were generated using CrystalExplorer21.5.³⁶

Conclusions

In conclusion, we have developed the electrophilic addition reaction of the TeBr₄ and aryltellurium tribromides C₆H₅TeBr₃, 4-MeOC₆H₄TeBr₃ and 1-C₁₀H₇TeBr₃ with terminal acetylene bonds of RC \equiv CH (R = Me₃C, C₆H₅, 4-MeC₆H₄), producing the respective (*Z*) isomer organotellurium(IV) derivatives **1–9**. These derivatives were characterized by elemental analysis, ¹H, ¹³C{¹H} and ¹²⁵Te{¹H} NMR spectroscopic techniques. Only one ¹²⁵Te NMR signal is observed for all the derivatives. Among these compounds, **2** and **7** were also characterized by single crystal X-ray studies.

Author contributions

Puspendra Singh: data curation, investigation, formal analysis, writing – original draft, Swami N. Bharti: methodology. Andrew Duthie: writing – review & editing. Ray J. Butcher: Single-crystal X-ray data and structure refinement.



Conflicts of interest

There are no conflicts to declare.

Data availability

Supplementary information (SI): additionally, the ^1H , $^{13}\text{C}\{^1\text{H}\}$, and $^{125}\text{Te}\{^1\text{H}\}$ spectrum are also included in the SI. See DOI: <https://doi.org/10.1039/d5ra07072d>.

CCDC 2482355 and 2482356 contain the supplementary crystallographic data for this paper.^{37a,b}

Acknowledgements

PS is heartily thankful to the Science and Engineering Research Board, New Delhi, India, for Teachers Associateship for Research Excellence Grant (Project No. TAR/2021/000075). PS and SNB are particularly grateful to Dr R. C. Srivastava and Dr Ashok K. S. Chauhan (Retired Professor of Department of Chemistry, University of Lucknow) for guidance and valuable suggestions. We are also thankful to Central Drug Research Institute Lucknow and Indian Institute of Technology Bombay for recording analytical data.

Notes and references

- 1 M. de M. Campos and N. Petragnani, *Tetrahedron*, 1962, **18**, 527.
- 2 S. M. Barros, M. J. Dabdoub, V. B. Dabdoub and J. V. Comasseto, *Organometallics*, 1989, **8**, 1661.
- 3 J. Zukerman-Schpector, H. A. Stefani, D. de O. Silva, A. L. Braga, L. Dornelles, C. da C. Silveira and I. Caracelli, *Acta Crystallogr.*, 1998, **C54**, 2007.
- 4 J. Zukerman-Schpector, I. Haiduc, M. J. Dabdoub, J. C. Biazotto, A. L. Braga, L. Dornelles and I. Caracelli, *Z. Kristallogr.*, 2002, **217**, 609.
- 5 (a) R. E. Barrientos-Astigarraga, P. Castelani, J. V. Comasseto, H. B. Formiga, N. C. da Silva, C. Y. Sumida and M. L. Vieira, *J. Organomet. Chem.*, 2001, **623**, 43; (b) G. Zeni, D. S. Lütke, R. B. Panatieri and A. L. Braga, *Chem. Rev.*, 2006, **106**, 1032.
- 6 A. L. Braga, C. C. Silveira, L. Dornelles, N. Petragnani and H. A. Stefani, *Phosphorus, Sulfur Silicon Relat. Elem.*, 2001, **172**, 181.
- 7 J. W. Sung, C. P. Park, J. M. Gil and D. Y. Oh, *Synth. Commun.*, 1998, **28**, 2635.
- 8 Y. Torubaev, A. A. Pasynskii and P. Mathur, *Russ. J. Coord. Chem.*, 2008, **34**, 805.
- 9 J. Zukerman-Schpector, H. A. Stefani, R. C. Guadagnin, C. A. Sukanuma and E. R. T. Tiekink, *Z. Kristallogr.*, 2008, **23**, 536.
- 10 A. Albeck, H. Weitman, B. Sredni and M. Albeck, *Inorg. Chem.*, 1998, **37**, 1704.
- 11 A. K. S. Chauhan, S. N. Bharti, R. C. Srivastava, R. J. Butcher and A. Duthie, *J. Organomet. Chem.*, 2012, **708–709**, 75.
- 12 X. Huang and Y.-P. Wang, *Tetrahedron Lett.*, 1996, **37**, 7417.
- 13 H. A. Stefani, N. Petragnani, J. Zukerman-Schpector, L. Dornelles, D. O. Silva and A. L. Braga, *J. Organomet. Chem.*, 1998, **562**, 127.
- 14 Y. Torubaev, P. Mathur and A. A. Pasynskii, *J. Organomet. Chem.*, 2010, **695**, 1300.
- 15 B. Singh, A. K. S. Chauhan, R. C. Srivastava, A. Duthie and R. J. Butcher, *RSC Adv.*, 2015, **5**, 58246.
- 16 I. C. Olanrewaju, S. R. Ponzo, A. K. Turner, H. E. Glover, F. R. Fronczek and T. Junk, *J. Organomet. Chem.*, 2025, **1035**, 123675.
- 17 K. M. Gaborit, A. K. Turner, S. R. Ponzo, F. R. Fronczek and T. Junk, *J. Organomet. Chem.*, 2024, **1020**, 123342.
- 18 S. R. Ponzo, F. R. Fronczek and T. Junk, *J. Organomet. Chem.*, 2024, **1003**, 122938.
- 19 M. H. Helal, A. Aljuhani and M. A. Gouda, *J. Organomet. Chem.*, 2024, **1020**, 123327.
- 20 R. Dhir and J. Dhau, *J. Organomet. Chem.*, 2024, **1006**, 123021.
- 21 (a) N. Petragnani and H. A. Stefani, *Tetrahedron*, 2005, **61**, 1613; (b) M. V. Musalova, V. A. Potapov and S. V. Amosova, *Russ. J. Org. Chem.*, 2016, **52**, 1842; (c) S. Uemura, H. Miyoshi and M. Okano, *Chem. Lett.*, 1979, **8**, 1357.
- 22 A. K. S. Chauhan, P. Singh, A. Kumar, R. C. Srivastava, R. J. Butcher and A. Duthie, *Organometallics*, 2007, **26**, 1955.
- 23 A. K. S. Chauhan, P. Singh, R. C. Srivastava, A. Duthie and A. Voda, *Dalton Trans.*, 2008, 4023.
- 24 S. Misra, A. K. S. Chauhan, P. Singh, R. C. Srivastava, A. Duthie and R. J. Butcher, *Dalton Trans.*, 2010, **39**, 2637.
- 25 A. K. S. Chauhan, S. N. Bharti, R. C. Srivastava, R. J. Butcher and A. Duthie, *J. Organomet. Chem.*, 2013, **728**, 38.
- 26 A. Bondi, *J. Phys. Chem.*, 1964, **68**, 441.
- 27 (a) P. Singh, M. Khan, A. Duthie and R. J. Butcher, *RSC Adv.*, 2024, **14**, 35650; (b) A. K. Tripathi, P. Singh, Anamika, J. K. Bera, A. Duthie and R. J. Butcher, *Polyhedron*, 2025, **272**, 117463.
- 28 (a) S. S. D. Santos, E. S. Lang and G. M. d. Oliveira, *J. Organomet. Chem.*, 2007, **692**, 3081; (b) P. Singh, A. K. Gupta, S. Sharma, H. B. Singh and R. J. Butcher, *Inorg. Chim. Acta*, 2018, **483**, 218.
- 29 W. R. McWhinnie and P. Thavornyutikarn, *J. Chem. Soc., Dalton Trans.*, 1972, 551.
- 30 N. Petragnani, *Tetrahedron*, 1960, **11**, 15.
- 31 Bruker, SAINT, Bruker AXS Inc., Madison, 2016.
- 32 SADABS, Area Detector Absorption Correction Program; Bruker Analytical X-ray, Madison, 2018.
- 33 G. M. Sheldrick, *Acta Crystallogr.*, 2015, **C71**, 3.
- 34 L. J. Farrugia, *J. Appl. Crystallogr.*, 2012, **45**, 849.
- 35 K. Brandenburg, and H. Putz, DIAMOND (v. 3.2e), Crystal Impact GbR, 1997–2012.
- 36 P. R. Spackman, M. J. Turner, J. J. McKinnon, S. K. Wolff, D. J. Grimwood, D. Jayatilaka and M. A. Spackman, *J. Appl. Crystallogr.*, 2021, **54**, 1006.
- 37 (a) CCDC 2482355: Experimental Crystal Structure Determination, 2025, DOI: [10.5517/ccdc.csd.cc2pb2z3](https://doi.org/10.5517/ccdc.csd.cc2pb2z3); (b) CCDC 2482356: Experimental Crystal Structure Determination, 2025, DOI: [10.5517/ccdc.csd.cc2pb305](https://doi.org/10.5517/ccdc.csd.cc2pb305).

